Sampling Strategies for Acoustic Holography/Holophony on the Sphere

Franz Zotter
Institute of Electronic Music and Acoustics, Email: zotter@iem.at,
University of Music and Performing Arts Graz, Austria.

Introduction

Discrete spherical microphone and loudspeaker arrays have been studied extensively for the purpose of sound field analysis and synthesis [4, 5, 6, 7, 9, 10, 13, 14]. For both, analysis and syntheis, the array patterns are decomposed into spherical base solutions by discrete spherical harmonics[1] transform (DSHT). This yields holographic/holophonic descriptions of the complete radiating or irradiating sound fields. Defining DSHT at finite order, it describes fields with uniformly limited angular resolution. Consequently, uniform angular sampling is required for DSHT, which turns out to be the nontrivial key issue for spherical arrays. In particular, the number of known regular sampling layouts is limited [19], and most constructive layouts [15, 22, 23, 24, 16, 27] may exhibit other limitations. It is generally advisable to take into account irregular sampling schemes optimized for their uniformity or for DSHT [18, 20, 21, 19, 23, 25]. Moreover, two side issues need to be addressed. Firstly, most arrays do not employ angular smoothing (anti-alias), thus suffer from angular aliasing. Aliasing has to be payed considerable attention [7, 6, 8], in order to reveal its impact on the field representation. Secondly, different sampling strategies may require different DSHT types, each of which having own properties. This paper characterizes different uniform sampling strategies on the sphere by their numerical DSHT condition, their sampling efficiency, and aliasing error. The ultimate challenge, non-uniform or incomplete sampling [26, 12, 11, 25] will not be covered here.

Definitions and Notation

Before defining the *discrete spherical harmoncis transform* (DSHT) for uniform discretization, the *spherical harmonics series* (SHS) and its discrete version (DSHS) is introduced, alongside with the notational conventions.

SHS. The SHS of the order N describes angularly band-limited functions $g(\boldsymbol{\theta})$ on the continuous sphere. Arranged by their indices n, m, all spherical harmonics (SH, [15, 2, 3]) $Y_n^m(\boldsymbol{\theta})$ of orders $n \leq \mathrm{N}$ can be written as an $(\mathrm{N}+1)^2 \times 1$ vector $\boldsymbol{y}_\mathrm{N}(\boldsymbol{\theta})$, the spherical angles denoted as $\boldsymbol{\theta}$. In this notation, the inner product of $\boldsymbol{y}_\mathrm{N}(\boldsymbol{\theta})$ with the expansion coefficients $\boldsymbol{\gamma}_\mathrm{N}$ yields the SHS

$$g(\boldsymbol{\theta}) = \boldsymbol{y}_\mathrm{N}(\boldsymbol{\theta})^\mathrm{T} \boldsymbol{\gamma}_\mathrm{N}, \tag{1}$$

with $$\boldsymbol{y}_\mathrm{N}(\boldsymbol{\theta})^\mathrm{T} = \left[Y_0^0(\boldsymbol{\theta}), Y_1^{-1}(\boldsymbol{\theta}), Y_1^0(\boldsymbol{\theta}), Y_1^1(\boldsymbol{\theta}), \ldots, Y_\mathrm{N}^\mathrm{N}(\boldsymbol{\theta})\right]. \tag{2}$$

[1]For a reference on spherical harmonics (SH), please refer to e.g. [1, 2, 3]. This paper uses a real-valued SH definition.

DSHS. The DSHS uses the coefficient vector $\boldsymbol{\gamma}_\mathrm{N}$ to represent a set of discrete samples $\{g(\boldsymbol{\theta}_l)\}$, exclusively. By stacking discretized SH-vectors Eq. (2) for all L sampling nodes into an $\mathrm{L} \times (\mathrm{N}+1)^2$ matrix $\boldsymbol{Y}_\mathrm{N}$, the DSHS yields the angular samples $\boldsymbol{g}$

$$\boldsymbol{g} = \boldsymbol{Y}_\mathrm{N}\, \boldsymbol{\gamma}_\mathrm{N}, \qquad \text{with } \boldsymbol{Y}_\mathrm{N} = \begin{bmatrix} \boldsymbol{y}_\mathrm{N}(\boldsymbol{\theta}_1)^\mathrm{T} \\ \vdots \\ \boldsymbol{y}_\mathrm{N}(\boldsymbol{\theta}_\mathrm{L})^\mathrm{T} \end{bmatrix}. \tag{3}$$

Exact DSHT. The DSHT is best defined as the inverse of the DSHS. It calculates unknown expansion coefficients $\boldsymbol{\gamma}_\mathrm{N}$ from the discrete angular samples $\boldsymbol{g}$. The inverse is symbolically denoted as $\boldsymbol{Y}_\mathrm{N}^{\text{"}-1\text{"}}$, because its particular type and existence may vary

$$\boldsymbol{\gamma}_\mathrm{N} = \boldsymbol{Y}_\mathrm{N}^{\text{"}-1\text{"}}\, \boldsymbol{g}. \tag{4}$$

Depending on the sampling strategy, several types of DSHT are considered:

- hyperinterpolation [21], $\boldsymbol{Y}_\mathrm{N}^{\text{"}-1\text{"}} = \boldsymbol{Y}_\mathrm{N}^{-1}$,
- (equally) weighted quadrature [15, 18, 19, 20, 22], $\boldsymbol{Y}_\mathrm{N}^{\text{"}-1\text{"}} = w\, \boldsymbol{Y}_\mathrm{N}^\mathrm{T}$, or $\boldsymbol{Y}_\mathrm{N}^{\text{"}-1\text{"}} = \boldsymbol{Y}_\mathrm{N}^\mathrm{T} \operatorname{diag}\{\boldsymbol{w}\}$,
- (weighted) least-squares [22, 26, 16, 24, 23, 17, 25], $\boldsymbol{Y}_\mathrm{N}^{\text{"}-1\text{"}} = \left(\boldsymbol{Y}_\mathrm{N}^\mathrm{T}\, \boldsymbol{Y}_\mathrm{N}\right)^{-1} \boldsymbol{Y}_\mathrm{N}^\mathrm{T}$, or $\boldsymbol{Y}_\mathrm{N}^{\text{"}-1\text{"}} = \left(\boldsymbol{Y}_\mathrm{N}^\mathrm{T} \operatorname{diag}\{\boldsymbol{w}\} \boldsymbol{Y}_\mathrm{N}\right)^{-1} \boldsymbol{Y}_\mathrm{N}^\mathrm{T} \operatorname{diag}\{\boldsymbol{w}\}$.

These types imply different requirements on the set of sampling nodes $\{\boldsymbol{\theta}_l\}$ on the sphere.

Sampling Characterization

The above listed DSHT types are suitable for different sampling strategies. *Hyperinterpolation* is the most *efficient* type, as all the array samples $\boldsymbol{g}$ are represented exactly using only $\mathrm{L} = (\mathrm{N}+1)^2$ sampling nodes.

Most sampling strategies are *inefficient*, as many of them require $\mathrm{L} > (\mathrm{N}+1)^2$ sampling nodes. In general, only approximate inversion of the over-determined system of DSHS equations is feasible. Note however, inversion is exact for samples $\boldsymbol{g}$ that fulfill angular band-limitation according Eq. (1). Although the implicit approximation has the effect of angular smoothing, its impact is not an angular anti-alias filter. All types of DSHT suffer from (angular) aliases, i.e. ambiguities, if the discretized function $g(\boldsymbol{\theta})$ is not band-limited.

Hyperinterpolation. Only highly special sets of nodes fulfill the strict requirement for the existence of the

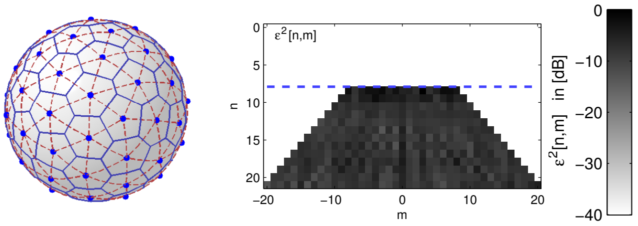

(a) Hyperinterpolation (*hi*) $\mathrm{L} = 64$, $\kappa = 15.4$

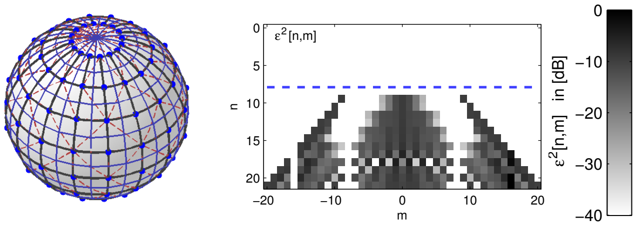

(b) Gauss-quadrature (*gl*) $\mathrm{L} = 128$, $\kappa = 1$

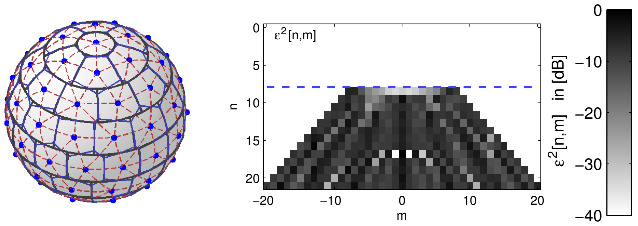

(c) Equal area partitions (*eq*) $\mathrm{L} = 75$, $\kappa = 2.7$

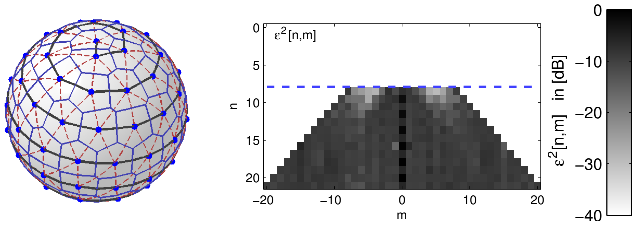

(d) Spiral points (*sp*) $\mathrm{L} = 76$, $\kappa = 16.4$

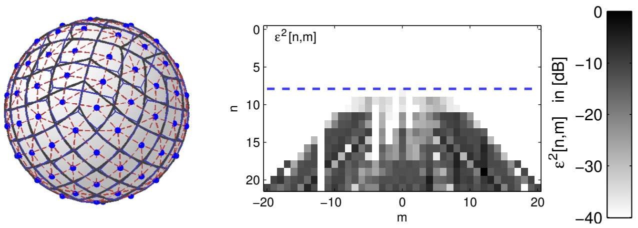

(e) HEALPix (*hp*) $\mathrm{L} = 108$, $\kappa = 1.7$

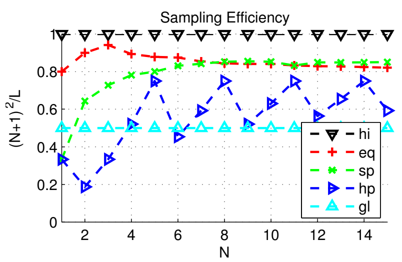

(f) Sampling Efficiency

Figure 1: Angular analysis aliasing maps following Rafaely *et al* [7] of sampling suitable for $\mathrm{N} = 7$, spheres plotted with CSTRIPACK viewer from Keiner [28]. The bottom diagram depicts the sampling efficiency of different samplings for the orders $1 \leq \mathrm{N} \leq 15$.

matrix inverse, cf. [21]. Hyperinterpolation is fully determined and exact for band-limited functions.

Quadrature requires the inner product $w\,\boldsymbol{Y}_\mathrm{N}^\mathrm{T}\,\boldsymbol{Y}_\mathrm{N} = \boldsymbol{I}$ (equally weighted), or $\boldsymbol{Y}_\mathrm{N}^\mathrm{T}\mathrm{diag}\{\boldsymbol{w}\}\,\boldsymbol{Y}_\mathrm{N} = \boldsymbol{I}$ (weighted), to indicate orthonormality. Only very few sampling layouts provide this orthonormality, most of which being over-determined $\mathrm{L} > (\mathrm{N}+1)^2$, cf. [15, 18, 19, 20, 22].

The *(weighted) least-squares* solution [22, 26, 27] does not require orthonormality of the over-determined $\mathrm{L} > (\mathrm{N}+1)^2$ DSHS system. For weighted least-squares

$$\left(\boldsymbol{g} - \boldsymbol{Y}_\mathrm{N}\,\gamma_\mathrm{N}\right)^\mathrm{T} \mathrm{diag}\left\{\boldsymbol{w}\right\}\left(\boldsymbol{g} - \boldsymbol{Y}_\mathrm{N}\,\gamma_\mathrm{N}\right) \rightarrow \min \qquad (5)$$

to be feasible, the sampling nodes must provide an existing inverse of $\left(\boldsymbol{Y}_\mathrm{N}^\mathrm{T}\,\mathrm{diag}\{\boldsymbol{w}\}\boldsymbol{Y}_\mathrm{N}\right)$. It is more flexible than quadrature, but still requires uniform sampling. In general, the order N for least-squares is best chosen as low as to provide a stable inverse. Unequal error weights $\boldsymbol{w}$ spatially re-shape the approximation error. Approximation with Voronoi-weights [27] unifies the angular error-distribution. Given quadrature nodes and weights, least-squares allows for higher analysis orders N than quadrature, in many cases.

Condition Number. The condition number [30] characterizes the feasibility of the DSHT with the given sampling nodes $\{\boldsymbol{\theta}_l\}$

$$\kappa = \mathrm{cond}\left\{\sqrt{\mathrm{diag}\{\boldsymbol{w}\}}\,\boldsymbol{Y}_\mathrm{N}\right\}. \qquad (6)$$

For orthonormal matrices $\kappa = 1$, and $\kappa > 1$ for matrices that are harder to invert. The condition number allows to chose a suitable order N for DSHT.

Sampling Efficiency. For a given L-point sampling set, we define the ratio between the largest number of harmonics $(\mathrm{N}+1)^2$, for which a stable DSHT is feasible $\kappa \leq \kappa_0$, and the number L as the *sampling efficiency*

$$E = \left(\mathrm{N}+1\right)^2/\mathrm{L}. \qquad (7)$$

$$\mathrm{N} \rightarrow \max : \mathrm{cond}\{\boldsymbol{Y}_\mathrm{N}\} \overset{!}{\leq} \kappa_0$$

$E = 1$ for *hyperinterpolation* and smaller for other methods. κ_0 may be chosen arbitrarily, according to the desired numerical stability.

Angular Aliasing on the Sphere. Angular analysis aliasing errors on the sphere are evaluated by transforming the DSHS of γ_Q at high-order $\mathrm{Q} \rightarrow \infty$ using a DSHT limited to N^th order. Ideally, the $n > \mathrm{N}$ order components should vanish, cp. [7]. The error is the deviation from this ideal, its square

$$\epsilon^2 = \gamma_\mathrm{Q}^\mathrm{T}\,\boldsymbol{E}_\mathrm{N,Q}^\mathrm{T}\,\boldsymbol{E}_\mathrm{N,Q}\,\gamma_\mathrm{Q}, \qquad (8)$$

$$\boldsymbol{E}_\mathrm{N,Q} = \boldsymbol{Y}_\mathrm{N}^{\text{"}-1\text{"}}\,\boldsymbol{Y}_\mathrm{Q} - \left(\boldsymbol{I},\,\boldsymbol{0}\right).$$

Angular synthesis aliasing errors are fairly similar, but use an equation with an N^th order steering vector $\boldsymbol{\gamma}_\mathrm{N}$

$$\epsilon^2 = \gamma_\mathrm{N}^\mathrm{T}\,\boldsymbol{E}_\mathrm{N,Q}\,\boldsymbol{E}_\mathrm{N,Q}^\mathrm{T}\,\gamma_\mathrm{N}. \qquad (9)$$

Angular Aliasing in the Acoustic Field. Aliasing in the acoustic field analysis (holography) or synthesis (holophony) requires a description deviating from the above, because radial propagation R_n occurs. In addition to sampling, the propagated aliasing depends on the array radius r_0 and the focus/projection radius r_p. Generically, the system of aliasing errors becomes

$$\boldsymbol{E}_{\mathrm{N,Q}} = \mathrm{diag}_{\mathrm{N}}\left\{R_n\right\} \boldsymbol{Y}_{\mathrm{N}}^{\text{"}-1\text{"}} \boldsymbol{Y}_{\mathrm{Q}}\, \mathrm{diag}_{\mathrm{Q}}\left\{R_n^{-1}\right\} - (\boldsymbol{I},\, \boldsymbol{0})\,,$$
$$\mathrm{diag}_{\mathrm{N}}\{R_n\} = \mathrm{diag}\{\mathrm{vec}_{\mathrm{N}}\{R_n\}\} = \mathrm{diag}\{[R_0,\, 0,\, \ldots \underbrace{R_n,\, \ldots,\, R_n}_{2n+1},\, \ldots,\, R_{\mathrm{N}}]^{\mathrm{T}}\}.$$

Typical examples for the propagation are given, suitable for different applications of discrete spherical arrays,

$$R_n = \begin{cases} \frac{\mathrm{i}}{\rho_0 c} \frac{h_n'(kr_p)}{h_n(kr_0)}, & \text{for radiation analysis (1)}, \\ \frac{\mathrm{i}}{\rho_0 c} \frac{h_n'(kr_0)}{h_n(kr_p)}, & \text{for radiation synthesis (2)}, \\ -k\, r_0^2\, \frac{h_n'(kr_0)}{h_n(kr_p)}, & \text{for irradiation analysis (3)}, \\ \frac{h_n(kr_p)}{h_n(kr_0)}, & \text{for irradiation synthesis (4)}, \end{cases}$$

in which the error $\boldsymbol{E}_{\mathrm{N,Q}}$ characterizes:

1. the aliased surface or sound particle velocity error on a closed vibrating sphere of the radius r_p, measured as radiated sound pressure at a concentric large and open spherical microphone array of the radius r_0.
2. the aliased sound pressure error at the radius r_p, radiated there by a concentric compact and closed spherical loudspeaker array with surface or sound particle velocity at the radius r_0.
3. the aliased error of a continuous spherical source distribution at the radius r_p, measured as irradiating sound pressure by a concentric small and closed spherical microphone array of the radius r_0.
4. the aliased error of a spherical continuous source distribution at the radius r_p, irradiated (projected) by a concentric large and open spherical loudspeaker array of the radius r_0.

Examples

Figs. 1 (a)–(e) gives examples of sampling sets for DSHT with $\mathrm{N} = 7$ fulfilling $\kappa \leq 1.2\kappa_{hi}$ of hyperinterpolation. In the left column the different sampling layout structures can be observed.

The right column shows the *angular aliasing* error map uses input patterns $\boldsymbol{\gamma}_{\mathrm{Q}}$ corresponding to the components $\gamma_{nm} = \delta_n\, \delta_m$, in accordance with [7]. The examples indicate the analysis errors caused by components $n > 7$. It also reveals the uniform aliasing error of *hyperinterpolation* and partial smoothing/cancellation of higher order components for other sampling techniques.

In terms of the *sampling efficiency* depicted in Fig. 1 (f) of various orders, hyperinterpolation sampling performs best. The equal area partitions [16, 17] and spiral points [16] seem to be efficient alternatives to hyperinterpolation [21].

Approximate DSHT

Approximate DSHT degrades holographic/holophonic computations. Nevertheless, this section provides supplementary information for cases with sampling that does not allow DSHT with satisfactorily high order. The following transform methods are considered

- regularized least-squares [26, 11], by pruning harmonics in $\boldsymbol{Y}_{\mathrm{N}}$ or by SVD, with the number of harmonics $\mathrm{N_h} \leq L$
  $\boldsymbol{Y}_{\mathrm{N}}^{\text{"}-1\text{"}} \approx \left(\boldsymbol{Y}_{\mathrm{N}}^{\mathrm{T}}\, \boldsymbol{Y}_{\mathrm{N}}\right)^{-1} \boldsymbol{Y}_{\mathrm{N}}^{\mathrm{T}},$
- exact sample match, minimum spectral power, or approximation with SVD for $L < (\mathrm{N}+1)^2$
  $\boldsymbol{Y}_{\mathrm{N}}^{\text{"}-1\text{"}} \approxeq \boldsymbol{Y}_{\mathrm{N}}^{\mathrm{T}} \left(\boldsymbol{Y}_{\mathrm{N}}\, \boldsymbol{Y}_{\mathrm{N}}^{\mathrm{T}}\right)^{-1},$
- direct transform [29], infinite order $\mathrm{N} \to \infty$.

Regularized least-squares is not exact anymore, but allows to approximate the inverse $\left(\boldsymbol{Y}_{\mathrm{N}}^{\mathrm{T}}\, \boldsymbol{Y}_{\mathrm{N}}\right)$, or $\left(\boldsymbol{Y}_{\mathrm{N}}^{\mathrm{T}}\, \mathrm{diag}\{\boldsymbol{w}\}\boldsymbol{Y}_{\mathrm{N}}\right)$, if it is ill-conditioned for the order N otherwise. The SVD (signular-value decomposition) [11], or pruning of linearly dependent base functions [26] provides *regularization.*

On the other hand, *exact sample match and minimum (weighted) spectral power* uses *minimization* of an underdetermined DSHS $\mathrm{L} < (\mathrm{N}+1)^2$. It is obtained by solving

$$\boldsymbol{\gamma}_{\mathrm{N}}^{\mathrm{T}}\, \mathrm{diag}\left\{\boldsymbol{\varpi}\right\} \boldsymbol{\gamma}_{\mathrm{N}} \to \min\,.$$
$$\text{s.t. } \boldsymbol{Y}_{\mathrm{N}}\, \boldsymbol{\gamma}_{\mathrm{N}} = \boldsymbol{g}$$

However, cavities appear between the angular samples, which approach 0 for $\mathrm{N} \to \infty$.

Direct transform by triangulation [29] uses infinite angular band-width and transforms linearly interpolated spherical triangles.

Conclusion

This paper gives a comprehensive overview of different sampling schemes on the sphere applicable to spherical acoustic holophony/holography, referencing available literature, and showing suitable types of discrete spherical harmonics transform (DSHT). Characterizations of efficient sampling, numerical stability, and aliasing errors have been presented, which are important for spherical array processing that relies on DSHT.

Furthermore, the terms *angular analysis/synthesis aliasing on the sphere / in the acoustic field* have been introduced. This allows for distinct descriptions of aliasing artifacts directly on the discretized sphere, and aliasing encountered in acoustic holography (analysis) and holophony (synthesis).

Some examples considering angular aliasing errors on the sphere and sampling efficiency have been given, and a generic formulation of aliasing in the acoustic field has been newly developed. Also, the existing approximate DSHT methods have been shown, referencing literature.

The graphical representation of holographic/holophonic aliasing in the acoustic field is a matter of future studies.

References

[1] N. A. Gumerov and R. Duraiswami: Fast Multipole Methods for the Helmholtz Equations in Three Dimensions. Elsevier, 1st ed., 2004.

[2] E. G. Williams: Fourier Acoustics. Academic Press, 1999.

[3] L. J. Ziomek: Fundamentals of Acoustic Field Theory and Space-Time Singal Processing. CRC Press, 1995.

[4] W. Song, W. Ellermeier, and J. Hald: Using beamforming and binaural synthesis for the psychoacoustical evaluation of target sources in noise. JASA, no. 123, pp. 910–924, 2008.

[5] S.-O. Petersen: Localization of Sound Sources Using 3D Microphone Array. M. thesis, University South Denmark, Odense, 2004.

[6] Z. Li: The Capture and Recreation of 3D Audio Scenes. PhD thesis, University of Maryland, 2005.

[7] B. Rafaely, B. Weiss, and E. Bachmat: Spatial Aliasing in Spherical Microphone Arrays. IEEE Transactions on Signal Processing, 55(3), 2007.

[8] F. Zotter, H. Pomberger, and M. Frank: An Alternative Ambisonics Formulation: Modal Source Strength Matching and the Effect of Spatial Aliasing. 126th AES Convention, Munich, 2009.

[9] A. Schlesinger, G. Del Galdo, J. Lotze, S. Husung, and B. Albrecht: Holographic Sound Field Analysis with a Scalable Spherical Microphone Array. 122nd AES Convention, Vienna, 2007.

[10] S. Moreau: Étude et réalisation d'outils avancés d'encodage spatial pour la technique de spatialisation sonore Higher Order Ambisonics: microphone 3D et contrôle de distance. PhD thesis, Université du Maine, 2006.

[11] J. Hannemann, K. D. Donohue: Virtual Sound Source Rendering Using a Multipole-Expansion and Method-of-Moments Approach. AES Journal, vol. 56, 2008.

[12] A. Sontacchi, F. Zotter, and R. Höldrich: 3D sound field rendering under non-idealized loudspeaker arrangements. Acoustics-08, Paris, 2008.

[13] V. Tarnow: Sound Radiation from Loudspeaker Systems with the Symmetry of the Platonic Solids. B&K Tech Report, 1974.

[14] R. Avizienis, A. Freed, P. Kassakian, and D. Wessel: A Compact 120 Independent Element Spherical Loudspeaker Array with Programmable Radiation Patterns. 120th AES Convention, San Francisco, 2006.

[15] J. R. Driscoll, and D. M. Healy Jr.: Computing Fourier Transforms and Convolutions on the 2-Sphere. Adv. Appl. Math., vol. 15, 1994.

[16] E. A. Rakhmanov, E. B. Saff, and Y. M. Zhou: Minimal Discrete Energy on the Sphere. Mathematical Research Letters, 1994.

[17] P. Leopardi: A Partition of the Unit Sphere into Regions of Equal Area and small Diameter. El. Trans. Num. Analysis, vol. 25, 2006.

[18] J. Fliege and U. Maier: A Two-Stage Approach for Computing Cubature Formulae for the Sphere. TR Math. Dortmund, 1996.

[19] R. H. Hardin, N. J. A. Sloane: McLaren's Improved Snub Cube and Other New Spherical Designs in Three Dimensions. Discr. Comp. Geometry, vol. 15, 1996.

[20] V. I. Lebedev: Spherical quadrature formulas exact to orders 25-29. Translated from Sibirskii Math. Zhurnal, vol. 18, 1977.

[21] R. S. Womersley and I. H. Sloan: How Good can Polynomial Interpolation on the Sphere be?. School of Mathematics, University New South Wales, Sydney, 2001.

[22] N. Sneeuw: Global Spherical Harmonic Analysis by Least-Squares and Numerical Quadrature Methods in Historical Perspective. Goeph. Journal Int., vol 118, 1994.

[23] K. M. Górski, et al.: HEALPix: A Framework for High-Resolution Discretization and Fast Analysis of Data Distributed on the Sphere. Astroph. Journal, vol. 622, 2005.

[24] K. Sahr, D. White, and A. J. Kimerling: Geodesic Discrete Global Grid Systems. Cart. and Geogr. Information Sc., vol. 30, 2003.

[25] Q. Du, M. D. Gunzburger, and L. Ju: Constrained Central Voronoi Tesselations for Surfaces. SIAM Journal Sc. Comp., vol. 24, 2003.

[26] R. Pail, G. Plank, and W.-D. Schuh: Spatially Restricted Data Distributions on the Sphere: the Method of Ortnonormalized Functions and Applications. Journal of Geodesy, vol. 75, 2001.

[27] J. Keiner, S. Kunis, and D. Potts: Efficient reconstruction of functions on the sphere from scattered data. J. Fourier Anal. Appl., vol. 13, 2007.

[28] J. Keiner: CSTRIPACK. C translation of Voronoi algorithm on the sphere, 2007, http://www.math.uni-luebeck.de/keiner/sonstiges.shtml

[29] M. Mousa, R. Chaine, and S. Akkouche: Direct Spherical Harmonic Transform of a Triangulated Mesh. Journal of Graphics Tools, vol. 11, 2006.

[30] Daniel Lichtblau and Eric W. Weisstein: Condition Number. From MathWorld, Wolfram, 2009, http://mathworld.wolfram.com/ConditionNumber.html